

Electrical properties of *in vitro* biomineralized recombinant silicatein deposited by microfluidics

Stefano Pagliara,^{1,a)} Alessandro Polini,^{1,b)} Andrea Camposeo,^{1,2} Heinz C. Schröder,³ Werner E. G. Müller,³ and Dario Pisignano^{1,2,4,c)}

¹National Nanotechnology Laboratory of Consiglio Nazionale delle Ricerche-Istituto Nanoscienze, Università del Salento, Via Arnesano, I-73100 Lecce, Italy

²Center for Biomolecular Nanotechnologies at UNILE, Fondazione Istituto Italiano di Tecnologia, Via Barsanti, I-73010 Arnesano, Italy

³Institute for Physiological Chemistry, Johannes Gutenberg University, Medical School, Duesbergweg 6, D-55099 Mainz, Germany

⁴Dipartimento di Matematica e Fisica "Ennio De Giorgi," Università del Salento, Via Arnesano, I-73100 Lecce, Italy

(Received 25 May 2012; accepted 22 October 2012; published online 8 November 2012)

We report the fabrication of silica dielectrics obtained by *in vitro* biomineralization of recombinant silicatein. We exploit pressure-driven microfluidics to deposit silicatein which catalyses the deposition of silica features with thickness in the range 2–6 μm . We follow the biomineralization process with staining and confocal fluorescence for an incubation time up to 5 days and correspondingly characterize the leakage current through the resulting biomineralized silica layer by embedding it into a metal-insulator-metal device. We further characterize the morphology of the biosilica surface through atomic force and scanning electron microscopy and demonstrate the electrical insulation within planar electrodes patterned over such surface with leakage currents in the pA range for applied bias up to tens of V. © 2012 American Institute of Physics. [<http://dx.doi.org/10.1063/1.4766186>]

Many efforts are spent today towards the low-cost realization of organic devices for microelectronics.^{1–6} Thin films of thermally evaporated low-molar-mass molecules or spin-cast conjugated polymers⁷ are employed as semiconducting layers in field-effect transistors (FETs), reaching carrier mobility comparable to those of hydrogenated amorphous silicon ($\geq 1 \text{ cm}^2/\text{Vs}$).^{4,6,8} Silicon dioxide still remains the most used dielectric material, though industrial processes for obtaining silica layers generally use toxic chemicals, and very high temperatures⁹ in extreme ranges of pHs and pressures, such as in chemical vapour deposition.¹⁰ For these and other^{1,3,4,7} reasons, spin-cast films of electrically inert polymers such as poly(vinyl alcohol),^{4,11} poly(vinyl phenol),^{2,12,13} and poly(methyl methacrylate) (PMMA)^{1,14} are employed as gate insulators, though adding further organic synthesis steps to the process. Other approaches are based on flexible ion gel dielectrics,¹⁵ sol-gel methods,¹⁶ or self-assembled SiO₂ nanoparticles.¹⁷ Biomaterials such as DNA-hexadecyltrimethylammonium chloride,¹⁸ nucleobases,¹⁹ silk,²⁰ and albumen²¹ have also been introduced as potential candidates for the upcoming low cost organic electronics since presenting the outstanding advantages of bioresorbability, biodegradability, and biocompatibility. Silica-based dielectric materials realized under mild, possibly physiological conditions^{22,23} via a low cost, high throughput and fully controlled technology would add value to the low-temperature processing and deposition methods of

organic semiconductors, which make these materials so attractive for a variety of applications. Microfluidics²⁴ is a well established approach that fully meets such requirements, it is easily predictable based on the analogous behaviour of hydraulic and electric circuits,²⁵ it enables the control of single species with size down to 50 nm²⁶ and it has been employed for the selective deposition of proteins.²⁷ Here, we introduce an approach toward the fabrication of continuous silica layers obtained by biomineralization of a recombinant silicatein deposited via microfluidics. We investigate the progress of the biomineralization process over the incubation time and we correspondingly characterize the quality of the resulting layers as electrically insulating media. We demonstrate electrical insulation with leakage currents down to the pA range under a bias of tens of V both across and on the surface of the biosilica layers thus being usable as dielectric layers for organic electronics.

The chance of combining oxide materials with the advantages of a soft technology for patterning silica layers is inspired by the nature. In fact, as opposed to conventional anthropogenic and industrial manufacturing, the biological synthesis of silica by several single- and multicellular organisms generally occurs at ambient temperature and pressure and at near-neutral pH through a process known as biomineralization.²⁸ In particular, sponges (phylum Porifera) produce complex silica skeletal architectures such as the spicules that provide structural support and protection to the animals and are highly diverse from species to species.²⁹ For instance, the marine demosponge, *Suberites domuncula* (Fig. 1(a)), exhibits spicules whose main fraction presents monaxonal tylostyles of hundreds of micrometers (Fig. 1(b)) terminating with a sharp tip and a knob with diameter of about 10 μm (inset in Fig. 1(b)). In this and other species,³⁰ the synthesis

^{a)}Present address: Cavendish Laboratory, University of Cambridge, J. J. Thomson Avenue, Cambridge CB3 0HE, United Kingdom.

^{b)}Present address: Lawrence Berkeley National Laboratory, Materials Sciences Division, 1 Cyclotron Road, Berkeley, California 94720, USA.

^{c)}Author to whom correspondence should be addressed. Electronic mail: dario.pisignano@unisalento.it.

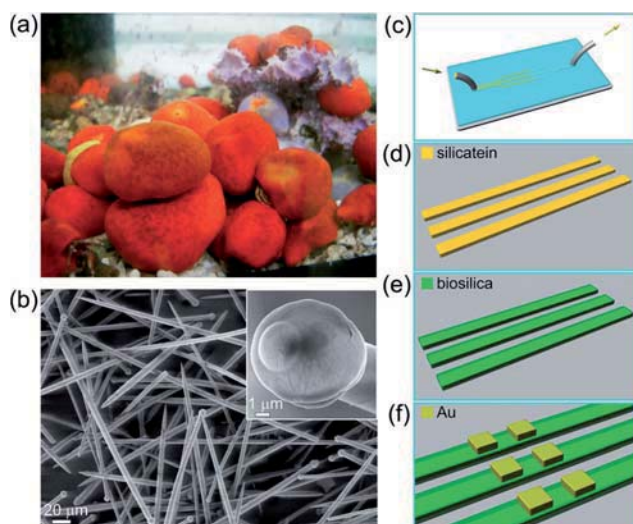


FIG. 1. The demosponge *Suberites domuncula* (a) and its spicules imaged by SEM (b). Inset of (b): knob at one of each spicule termini. (c)–(g) Electronics on biosilica. Schematics of silicatein features patterning via pressure-driven microfluidics (c–d), biosilica growth during incubation in TEOS (e), and Au electrode patterning (f). Features not in scale.

of biosilica is catalysed by a specific protein, namely the silicatein,³¹ belonging to the cathepsin proteinase family.³⁰ Not only does enzymatically generated biosilica show optical properties similar to those of artificial optical fibers for confining and guiding light,³² but, as here demonstrated, it can also serve as dielectrics. Silicatein extracted from this and other natural sources, such as the sponges *Petrosia ficiformis* and *Tethya aurantia*,^{30–33} is a complex protein, subjected to post-translational modifications, and has a high enzymatic activity. However, important requirements for the exploitation of biosilica coatings as dielectrics are large area patterning ability, high throughput, and mass production. These aspects suggest the use of recombinant proteins which show a good enzymatic activity,^{22,23,30,34} thus overcoming issues related to laborious and low-throughput isolation from natural sources, and the sacrifice of living organisms.

The patterning of biogenic silica features is schematized in Figs. 1(c)–1(f). Recombinant silicatein is deposited on a Si substrate by external pumping into the hollow microchannels of a system composed of an elastomeric mold, replicating a photolithographically realized master and placed in conformal contact with the substrate (Fig. 1(c)). Masters for defining the microfluidic devices and for protein patterning are realized by photoresist deposition (SU8), UV-exposure (20'' at 350 W), and development. Typical master features are 1000 μm in width and 2–6 μm in thickness (as measured by a Dektak stylus profilometer) controlled by employing photoresists of different viscosities and with different spin-coating rates. An elastomeric replica of the master is obtained by *in situ* polymerization (75 °C, 20') of poly(dimethylsiloxane) (PDMS, A:B 1:4). Such replica is then placed onto the surface of n-type Si wafers.

The hydrophobic nature and poor wettability of pristine PDMS are well documented its water contact angle being around 120° (Ref. 35) while bare silicon presents a partial hydrophilic character and a contact angle around 35°.³⁶ The spontaneous filling of such microchannels with mixed hydro-

philic and hydrophobic walls has been previously investigated³⁷ resulting in only a partial filling of the channel. The most used approach to overcome this issue relies in the plasma and chemical treatment of the involved surfaces to improve their wettability;^{35,38} however, this often results in microchannel sealing. On the other hand, pressure driven microfluidics offers a full control over the capillary filling. We use a programmable peristaltic syringe pump (Harvard Apparatus) connected to the microfluidic chip via a series of plastic tubing and shut off valves for inlet and outlet fluidic access and flow stopping, and find an optimal injection flow rate in the range of 50–100 $\mu\text{l}/\text{h}$. Exploring various flow rates, we establish the above range as the best compromise between faithful pattern transfer to silicatein (width is fully transferred while thickness is reproduced up to its 90%) and process yield (a series of parallel microchannels are simultaneously filled in a few seconds). A quantity of 2 μl of silicatein solution (0.85 mg/ml, full details about the preparation of recombinant silicatein are reported elsewhere³⁴) is enough to completely fill the whole chip.

After 2 h being the evaporation of the solvent complete, the elastomeric replica is peeled off and the Si substrate with silicatein features is incubated in tetraethyl orthosilicate (TEOS) solution for 24–120 h for silica biomineralization (Fig. 1(d)). The biomineralization process is followed with staining and confocal fluorescence as reported elsewhere.²² Briefly, biosilica patterned substrates are incubated in a R123 solution at a concentration of 1 $\mu\text{g}/\text{ml}$ in phosphate buffer solution (PBS) for 24 h, and washed three times with PBS. The investigation is carried out by confocal laser scanning microscopy equipped with an Ar laser source using 488 nm as excitation wavelength. The detected fluorescence intensity increases monotonously with the TEOS incubation time (Figs. 2(a)–2(c)). The polycondensation of the precursor, catalytically directed by silicatein and resulting in precipitating silica, induces important changes in the physical properties of the final film with respect to the pristine protein layer. In order to investigate the resulting electrical properties, conductivity measurements are carried out on both native silicatein and biomineralized features after incubation in TEOS for different time intervals (up to 120 h). Au electrodes are deposited on the biomineralized surface by physical vapour deposition through shadow masks (copper grids with 25 μm -wide bars and square holes with side of 75 μm , Fig. 1(f)), and a further electrical contact is realized on the highly doped silicon substrate. The electrical characterization is carried out by manual miniature probeheads, a semiconductor parameter analyzer (4200 SCS, Keithley Instruments), and a stereomicroscope for device visual inspection and careful probe positioning. Each micrometric probehead is connected to a W probe tip to carefully contact the device terminals. Si is contacted by a probe tip on a Cu plate, on its turn placed under the substrate. The different electrical response of Au, Si and Cu and eventual local faulty contacts between Si and Cu surfaces may result in the registration of non-zero currents under zero applied bias. These current values are generally comparable with instrumental sensitivity. Silicatein structures carry current densities (J) up to the order of A cm^{-2} , whereas the biosilica ones formed after 120 h of incubation are characterized by J values below

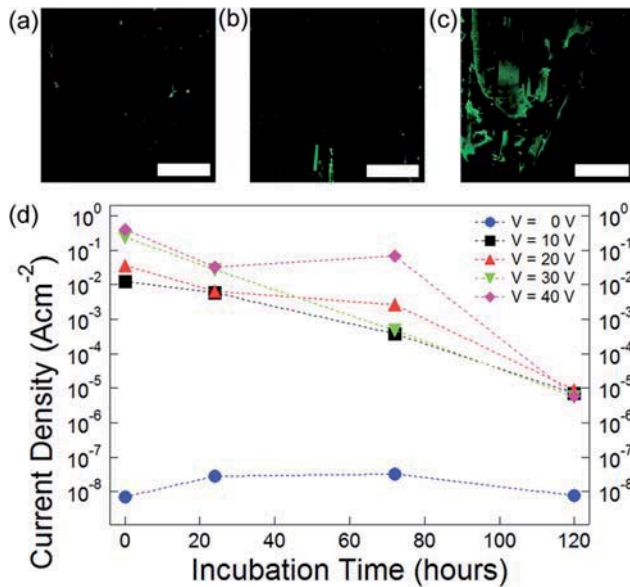


FIG. 2. Growth and characterization of the biosilica layer. (a)–(c) Confocal fluorescence micrographs of silica films labeled by Rh123, after a TEOS incubation time of 0 (a), 48 h (b), and 72 h (c). Excitation provided by an Ar laser (488 nm). Scale bar: $100\ \mu\text{m}$. (d) Currents through the biomaterialized layer vs. incubation time, as measured in a metal-insulator-semiconductor configuration under an applied bias of 0 (circles), 10 (squares), 20 (upward triangles), 30 (downward triangles), and 40 V (rhombus).

$10^{-5}\ \text{A cm}^{-2}$ (Fig. 2(d)). The clear enhancement of the insulating properties of biosilica upon increasing the incubation time is consistent with the formation and progressively proceeding aggregation of silica particles³⁹ as induced by the silicatein, finally filling nanoscale voids in the dielectric layer.

The surface of such dielectrics is investigated by scanning electron microscopy (SEM) using an accelerating voltage of 2 kV and an aperture size of $30\ \mu\text{m}$ revealing a uniform surface (Fig. 3(a)) over areas up to $0.3\ \text{mm}^2$. Atomic force microscopy (AFM) reveals a surface root mean square roughness value of about 4 nm over several $100\ \mu\text{m}^2$ areas (Fig. 3(b)).

We explore dielectrics with thickness in the range 2–6 μm . In fact, we find that the thickness (Z) of each biomaterialized feature is strongly affected by the one of the silicatein deposited by microfluidics (thickness variation smaller than 10% as measured by a stylus profilometer), and thus ultimately related to the height of the used microchannels. Controlling the geometry of the elastomeric elements by properly realized master patterns, these layers are obtainable with Z values tuneable between 2 and 6 μm after 120 h of TEOS incubation. On 6 μm -thick layers, the average measured J values are stable around a few nA cm^{-2} under applied electric fields below $10\ \text{kV cm}^{-1}$, increasing up to the range of $\mu\text{A cm}^{-2}$ above $500\ \text{kV cm}^{-1}$. The current density increases by four orders of magnitude (up to $10^{-4}\ \text{A cm}^{-2}$ at an applied bias of 30 V) upon decreasing Z from 6 to 2 μm (Fig. 4(a)). For sake of comparison, 2 μm -thick biomaterialized layers carry J values higher by about one order of magnitude with respect to 1 μm -thick spin-cast PMMA under comparable applied electric fields (Fig. 4(b)).

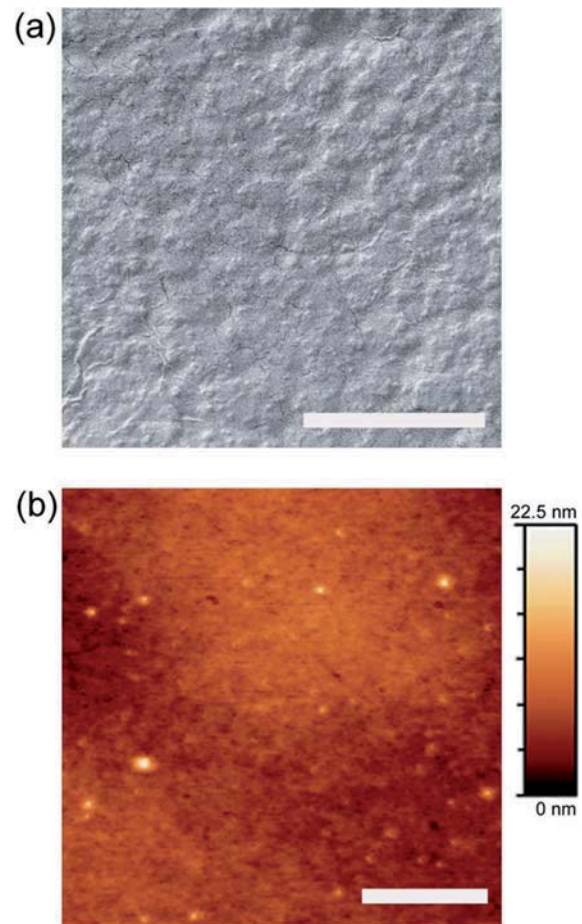


FIG. 3. Biosilica surface morphology imaged by SEM (a) and AFM (b), after 120 h of TEOS incubation. Scale bars: 20 and $1\ \mu\text{m}$ for (a) and (b), respectively.

Overall biosilica films can be promising as dielectrics for organic electronics. In fact, the electrical insulation between two electrical contacts deposited on the surface of each biosilica feature (circles in Fig. 4(c), electrodes at a reciprocal distance of $20\ \mu\text{m}$ as shown in Fig. 4(c) inset) is measured to be as good as the one measured across the biosilica layers (squares) with leakage currents of less than 1 pA for applied bias up to 30 V.

The full viability of this approach would need thinner and smooth, ultimately 100 nm-scale, biomaterialized layers. We anticipate that this can be accomplished in future by the inclusion of small amounts of TEOS ($\sim 10\%$ in volume) in the silicatein solution during the surface functionalization step. Preliminary experiments in this sense demonstrate the possibility of speeding up the biosilica formation, and to favour the formation of biosilica layers with reduced thickness (down to about 1 μm). Indeed, the presence of silica precursors in the patterned silicatein film is likely to promote the fusion and interconnection of small silica particles during the incubation.³⁹

It is noteworthy to observe that the presented biosilicification approach offers a valid alternative toward the production of natural biogenic silica films under physiological conditions by mimicking the capabilities of single- and multicellular organisms to realize species-specific 2D and

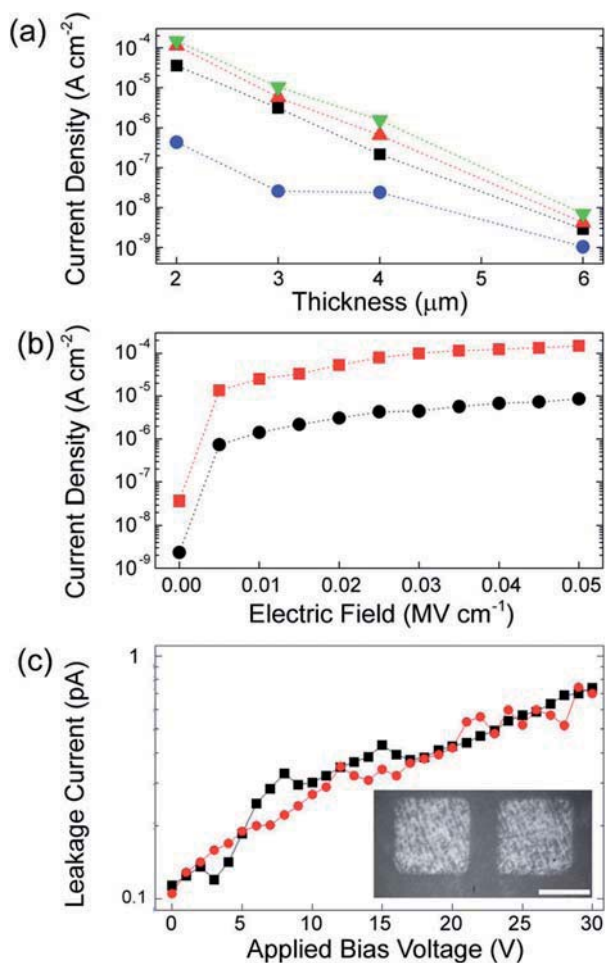


FIG. 4. Leakage currents. (a) Measured current density, across the biosilica layer as a function of its thickness under an applied voltage, V_{GS} , of 0 (circles), 10 (squares), 20 (upward triangles), and 30 V (downward triangles) (with $V_{DS} = -40$ V). (b) Current density through 2 μm -thick biosilica (squares) and 1 μm -thick PMMA (circles) vs. applied electric field. (c) Leakage current on the surface (circles) and across the thickness (squares) of a biosilica feature. Inset: micrograph of $75 \times 75 \mu\text{m}^2$ Au electrodes patterned on the surface of a biosilica feature at a reciprocal distance of 20 μm . Scale bar: 50 μm .

3D nano- and microstructures. Other low-temperature approaches such as sol-gel chemistries,⁴⁰ may still involve the exploitation of acidified solutions, alcohols, surfactant species, and heating (at 100 °C) to initiate the gelation step or during the post-processing phase.^{16,40}

In summary, we fabricate biogenic silica dielectrics by exploiting microfluidics and biomineralization in silica precursors and correlate the morphological, chemical, and electrical properties of such layers with respect to the incubation time. We show that biosilica layers exhibit electrically insulating properties both across their thickness and above their surface, with leakage currents in the pA range for applied bias up to tens of V. Combining microfluidics and biomineralization offers the chance for *in situ* selective patterning of dielectrics, under physiological conditions and in a fully controlled microenvironment for disposable electronics and sensing.

We gratefully acknowledge the support from the BIO-LITHO European project (6th Framework Program, NMP).

W.E.G. Müller is holder of an ERC Advanced Research Grant.

- ¹M. Muccini, *Nature Mater.* **5**, 605 (2006).
- ²S. J. Kim and J.-S. Lee, *Nano Lett.* **10**, 2884 (2010).
- ³C. J. Bettinger and Z. Bao, *Adv. Mater.* **22**, 651 (2010).
- ⁴G. Gelincik, P. Heremans, K. Nomoto, and T. D. Anthopoulos, *Adv. Mater.* **22**, 3778 (2010).
- ⁵M. A. McCarthy, B. Liu, E. P. Donoghue, I. Kravchenko, D. Y. Kim, F. So, and A. G. Rinzler, *Science* **332**, 570 (2011).
- ⁶A. C. Arias, J. D. Mackenzie, I. McCulloch, J. Rivnay, and A. Salleo, *Chem. Rev.* **110**, 3 (2010).
- ⁷H. Klauk, *Chem. Soc. Rev.* **39**, 2643 (2010).
- ⁸H. Yan, Z. Chen, Y. Zheng, C. Newman, J. R. Quinn, F. Dötz, M. Kastler, and A. Facchetti, *Nature* **457**, 679 (2009).
- ⁹K. H. Büchel, H. H. Moretto, and P. Woditsch, *Industrial Inorganic Chemistry* (Wiley-VCH, Weinheim, Germany, 2000).
- ¹⁰R. Doering and Y. Nishi, *Handbook of Semiconductor Manufacturing Technology* (CRC, USA, 2007).
- ¹¹Th. B. Singh, F. Meghdadi, S. Günes, N. Marjanovic, G. Horowitz, P. Lang, S. Bauer, and N. S. Sariciftci, *Adv. Mater.* **17**, 2315 (2005).
- ¹²C. A. Lee, D.-W. Park, K.-D. Jung, B.-J. Kim, Y. C. Kim, J. D. Lee, and B.-G. Park, *Appl. Phys. Lett.* **89**, 262120 (2006).
- ¹³M. Halik, H. Klauk, U. Zschieschang, G. Schmid, W. Radlik, and W. Weber, *Adv. Mater.* **14**, 1717 (2002).
- ¹⁴J. H. Park, D. K. Hwang, J. Lee, S. Im, and E. Kim, *Thin Solid Films* **515**, 4041 (2007).
- ¹⁵J. H. Cho, J. Lee, Y. Xia, B. Kim, Y. He, M. J. Renn, T. P. Lodge, and C. D. Frisbie, *Nature Mater.* **7**, 900 (2008).
- ¹⁶A. R. Abate, D. Lee, T. Do, C. Holtze, and D. A. Weitz, *Lab Chip* **8**, 516 (2008).
- ¹⁷T. Cui and G. Liang, *Appl. Phys. Lett.* **86**, 064102 (2005).
- ¹⁸Y. S. Kim, K. H. Jung, U. R. Lee, K. H. Kim, M. H. Hoang, J.-I. Jin, and D. H. Choi, *Appl. Phys. Lett.* **96**, 103307 (2010).
- ¹⁹M. Irimia-Vladu, P. A. Troshin, M. Reisinger, G. Schwabegger, M. Ullah, R. Schwoedlauer, A. Mumyatov, M. Bodea, J. W. Fergus, and V. F. Razuvov, *Org. Electron.* **11**, 1974 (2010).
- ²⁰C.-H. Wang, C.-Y. Hsieh, and J.-C. Hwang, *Adv. Mater.* **23**, 1630 (2011).
- ²¹J.-W. Chang, C.-G. Wang, C.-Y. Huang, T.-D. Tsai, T.-F. Guo, and T.-C. Wen, *Adv. Mater.* **23**, 4077 (2011).
- ²²A. Polini, S. Pagliara, A. Camposeo, A. Biasco, H. C. Schröder, W. E. G. Müller, and D. Pisignano, *Adv. Mater.* **23**, 4674 (2011).
- ²³A. Polini, S. Pagliara, A. Camposeo, R. Cingolani, X. Wang, H. C. Schröder, W. E. G. Müller, and D. Pisignano, *Sci. Rep.* **2**, 607 (2012).
- ²⁴V. Tesar, *Pressure-Driven Microfluidics* (Artech House, Boston, 2007).
- ²⁵K. W. Oh, K. Lee, B. Ahna, and E. P. Furlani, *Lab Chip* **12**, 515 (2012).
- ²⁶S. Pagliara, C. Chimere, R. Langford, D. G. A. L. Aarts, and U. F. Keyser, *Lab Chip* **11**, 3365 (2011).
- ²⁷J. Yakovleva, R. Davidsson, M. Bengtsson, T. Laurell, and J. Ennéus, *Biosens. Bioelectron.* **19**, 21 (2003).
- ²⁸E. Bäuerlein, *Biomineralization* (Wiley-VCH, Weinheim, Germany, 2004).
- ²⁹X. Wang, M. Wiens, H. C. Schröder, S. Hu, E. Mugnaioli, U. Kolb, W. Tremel, D. Pisignano, and W. E. G. Müller, *Adv. Eng. Mater.* **12**, B422 (2010).
- ³⁰J. N. Cha, K. Shimizu, Y. Zhou, S. C. Christiansen, B. F. Chmelka, G. D. Stucky, and D. E. Morse, *Proc. Natl. Acad. Sci. U.S.A.* **96**, 361 (1999).
- ³¹K. Shimizu, J. Cha, G. D. Stucky, and D. E. Morse, *Proc. Natl. Acad. Sci. U.S.A.* **95**, 6234 (1998).
- ³²R. Cattaneo-Vietti, G. Bavestrello, C. Cerrano, M. Sarà, U. Benatti, M. Giovine, and E. Gaino, *Nature* **383**, 397 (1996).
- ³³A. Armirotti, G. Damonte, M. Pozzolini, F. Mussino, C. Cerrano, A. Salis, U. Benatti, and M. Giovine, *J. Proteome Res.* **8**, 3995 (2009).
- ³⁴U. Schloßmacher, M. Wiens, H. C. Schröder, X. Wang, K. P. Jochum, and W. E. G. Müller, *FEBS J.* **278**, 1145 (2011).
- ³⁵D. Bodas and C. Khan-Malek, *Microelectron. Eng.* **83**, 1277 (2006).
- ³⁶K. L. Osborne III, "Temperature-dependence of the contact angle of water on graphite, silicon, and gold," M.S. thesis (Worcester Polytechnic Institute, 2009).
- ³⁷V. Jokinen and S. Franssila, *Microfluid. Nanofluid.* **5**, 443 (2008).
- ³⁸D. Pisignano, F. Di Benedetto, L. Persano, G. Gigli, and R. Cingolani, *Langmuir* **20**, 4802 (2004).
- ³⁹C. C. Perry, *Rev. Mineral. Geochem.* **54**, 291 (2003).
- ⁴⁰S. V. Patwardhan, *Chem. Commun.* **47**, 7567 (2011).